Adaptive evolution drives the diversification of zinc-finger binding domains.

Deena Schmidt and Rick Durrett*,

Center for Applied Mathematics and Department of Mathematics

Cornell University

Key words: tandem gene duplication, adaptive evolution, zinc-finger genes

Running Head: Adaptive evolution of zinc-finger genes

* Corresponding Author: 523 Malott Hall, Cornell U. Ithaca NY 14853

Phone: (607) 255-8282, FAX: 255-7149, email: rtd1@cornell.edu

ABSTRACT

The human genome is estimated to contain 700 zinc finger genes, which perform many key functions including regulating transcription. The dramatic increase in the number of these genes as we move from yeast to *C. elegans* to Drosophila and to humans, as well as the clustered organization of these genes in humans suggests that gene duplication has played an important role in expanding this family of genes. Using likelihood methods developed by Yang and parsimony methods introduced by Suzuki and Gojobori, we have investigated four clusters of zinc finger genes on human chromosome 19 and found evidence that positive selection was involved in diversifying the family of zinc finger binding motifs.

INTRODUCTION

In the human genome there are hundreds of zinc finger genes organized into more than a dozen different families. (Gell, Crossley, and Mackay 2003). Here, we will concentrate on the C_2H_2 type, a 28 amino acid motif that is named for the two Cysteines and two Histidines that form a tetrahedral complex around a zinc ion to produce the finger structure (Miller, McLachan, and Klug 1985). See Figure 1. Zinc fingers are tandemly repeated at the end of zinc finger genes. The number of repeats ranges from two up to three dozen or more. In rodents and in humans about one third of the zinc finger genes carry the Krüppel-associated box (KRAB), a potent repressor of transcription (Margolin et al. 1994), which is named for the Drosophila segmentation gene *Krüppel* (Schuch, Aichler, and Gaul 1986, Bellefroid et al. 1991). There are more than 200 KRAB containing zinc finger genes in the human genome, about 40% of which reside on chromosome 19 and show a clustered organization suggesting an evolutionary history of duplication events (Dehal et al. 2001).

The total number of zinc finger genes appears to have increased through evolution. There are 564-706 in humans compared to 234-357 in *D. melanogaster*, 68-151 in *C. elegans*, and 34-48 in *S. cerevisiae*. (Lander et al. 2001 and Venter et al. 2001). The average number of fingers per gene has increased, being 8, 3.5, 2.5, and 1.5 respectively in the four species just mentioned (Looman 2003).

In addition to a general increase in the number of zinc finger genes, some regions of the human genome contain many such genes with no homologs in rodents. Bellefroid et al. (1995) studied the ZNF91 gene family on human chromosome 19p12-p13.1. They found ZNF91 family members in a number of primate species but could find no murine

gene with sequence similarity to ZNF91. They concluded that this cluster resulted from duplication events some 55 million years ago.

The structure and binding properties of zinc finger genes have been extensively studied, see Wolfe, Nekludova, and Pabo (1999) for a review. A C_2H_2 zinc finger consists of an α-helix that begins between the first two asterisks in Figure 1 and continues to the first Histidine. The remainder of the finger consists of two anti-parallel β sheets. The amino acids at positions -1, 3, and 6 with respect to the α-helix make contacts to bases 3, 2 and 1 in the primary DNA strand, whereas the amino acid at α-helix position 2 makes contact to the complement of base 4. The recognition code for zinc finger binding has been widely studied (Choo and Klug 1997). However recent research (Benos, Lapedes, and Stromo 2002) suggests that no simple 1-1 relationship exists, but that different amino acid sequences bind to target nucleotide sequences with different efficiencies.

The H/C link TGEKPY/F separating adjacent fingers (dark gray in Figure 1), the two C and two H positions bound to the zinc atom to make the finger, as well as the hydrophobic Phenyalanine (F) and Leucine (L) are highly conserved. However, the four sites involved in binding the protein to DNA indicated by asterisks in Figure 1 are highly variable.

These observations and the fact that even closely related genes display distinct patterns of tissue-specific expression (Shannon et al. 2003) suggest that gene duplication has aided in the diversification of zinc finger binding motifs. Shannon et al. (2003) used pairwise d_N / d_S comparisons to examine selective pressures in what we will call clusters I and II below. The goal of this paper is to use the methods of Yang et al. (2000), Yang

and Swanson (2002), and Suzuki and Gojobori (1999) to look for signs of positive selection in these clusters and others on human chromosome 19.

MATERIALS AND METHODS

Using the Human Genome Resources on the NCBI web site http://www.ncbi.nlm.nih.gov/genome/guide/human/ we downloaded sequences for all genes on chromosome 19 that were described as zinc finger genes. In regions where these genes clustered we examined the Locus Link entries for nearby predicted genes and included those annotated as having C_2H_2 zinc fingers or KRAB domains, resulting in a total of 173 genes. To complete our data set, we found the annotated mouse (29) and rat (20) orthologs of the human genes.

To examine the relationship between zinc finger genes, we aligned the KRAB domains and spacer sequences of our genes using ClustalW. We did not use the zinc fingers in the alignment because the number varied considerably between genes, and the repetitive zinc finger structure resulted in the alignment of fingers with much dissimilarity. Alignments were done using the European Bioinformatics Institute's server (http://www.ebi.ac.uk/clustalw/) with default parameters. As described in Thompson, Higgins, and Gibson (1994), ClustalW (i) performs a pairwise alignment of all sequences, (ii) computes a distance matrix based on the percentage of identities between the two aligned sequences, (iii) produces a tree by the neighbor joining algorithm and then (iv) uses the tree to guide the multiple alignment.

Using the clustering of genes on the tree and a comparison of their α-helix sequences (see results for more details) we identified four sets of genes for study. For each gene cluster we obtained the mRNA sequences from the NCBI web site and located the fingers that were common to all of the genes to make our comparison data set. In each case, alignment of the selected fingers using ClustalW resulted in an alignment with no gaps in any sequence, and trees that agreed with those that had been constructed from the alignment of KRAB domains and spacer sequences. To further confirm the phylogenies, we built trees using parsimony and neighbor joining methods implemented in PHYLIP using the web server at http://bioweb.pasteur.fr/seqanal/phylogeny/phylip-uk.html. In clusters II-IV, the trees from all methods were identical. In cluster I, we found two tree topologies that differed in the positions of ZNF 224 and 225 which are almost equidistant from the pair ZNF 155 and 221, so we analyzed this cluster under both trees. Results of subsequent tests were very similar for the two trees. To look for signs of positive selection in our four clusters, we used the following three approaches.

Site-specific models. Nielsen and Yang (1998) and Yang et al. (2000) introduced various models to study how the distribution of $\omega = d_N/d_S$ varies along sequences. Model M7 has an ω for each site drawn from a beta distribution with parameters p and q. Model M8 uses the M7 recipe for a fraction p_0 of the sites and assigns another ω to the remaining fraction. M7 and M8 are nested models so they can be compared using a likelihood ratio test (LRT). Twice the difference in log likelihood between models is compared with the value obtained under a χ^2 distribution with degrees of freedom equal to the difference in number of parameters between models (in this case 2). When M8 fits the data significantly better than M7 and the ω ratio estimated under model M8 is greater

than 1, we need to ask if it is significantly greater than 1. To do this, we recalculate the log likelihood value in M8 while fixing ω to be 1 (model M8A from Swanson et al. 2003), and compare the change in likelihood with a χ^2 distribution with one degree of freedom.

Fixed-sites models. The approach in the last paragraph does not take into account the fact that zinc fingers are periodic, so we will also use a method developed by Yang and Swanson (2002) that allows us to take advantage of a priori knowledge. We divide the sites into 3 classes: constrained sites (finger positions 1, 2, 4, 7, 11, 17, 20, 24, 25, 26, 27, 28), the binding sites (13, 15, 16, 19), and the remaining "unconstrained" sites. We have used quotation marks since it will turn out that these sites have ω's significantly smaller than 1.

Let κ be the transition/transversion ratio, π_i the frequency of amino acid *i,* and let r_j denote the ratio of substitution rates for the *j*th site class to that of the first, with $r_1 = 1$. Yang and Swanson (2002) introduced the following models. In model A, there is only one rate class and all sites use the same κ, ω, and π's. In model B, the *r*'s are different but all sites use the same κ, ω, and π's. In model C, the *r*'s and π's are different, but all sites use the same κ and ω. In model D, the *r*'s, κ's, and ω's are different, but all sites use the same π's. In model E, each class has a different set of parameters. In model F, the sites are divided into three groups and analyzed separately. Tests were carried out using version 3.14 of PAML, software introduced by Yang (1997).

Parsimony analysis. Finally, at the request of two referees, we used Suzuki and Gojobori's (1999) method as implemented in ADAPTSITE.p version 1.3 (http://mep.bio.psu.edu/adaptivevol.html) to look for positive selection in our four

clusters. The test is based on comparing the observed total number of synonymous (s_c) and nonsynonymous (n_c) substitutions for a codon, to the Binomial with t_c trials and success probability p, where t_c is the total number of changes and p is the fraction of synonymous changes expected in the tree. There are several reasons not to use this test. The first is that the distribution of s_c conditioned on the observed values of t_c and p is not Binomial, see Durrett (2004). The second is that the test has very low power unless the number of sequences compared is large, see Wong et al. (2004). Suzuki and Gojobori (1999) say that a tree length of at least 2.5 nucleotide changes per codon site is needed to detect positive selection. Adding the branch lengths of the maximum parsimony trees shows that our clusters range from 0.45 to 0.6 changes per site. However, we can remedy this problem by taking advantage of the periodic structure of zinc finger genes and grouping codons together by position in the 9-10 fingers being compared. This is similar to our second PAML analysis but now our groups are the 28 finger positions rather than the 3 classes of sites. Due to our a priori beliefs, we performed one tailed tests of positive selection at the four binding sites and of negative selection at the other sites.

RESULTS

Statistical analysis. Figure 2 displays a histogram of the number of zinc fingers, defined as a sequence of 28 amino acids having C's, H's, F's and L's in the expected location. The average number of fingers for genes in our data set is 10.92. The five genes with the largest number are LOC126502(28), LOC25893(29), ZNF91(31), LOC126494(34), and its mouse ortholog MMU380856(30). Here and in what follows we

will replace LOC in the name of mouse and rat genes by MMU and RNO to make it clear what species they come from.

Table 1 gives amino acid usage by position in the finger. Numbers at the top of each column refer to the positions and letters in the second row of each column give the predicted residue for each location, with *'s indicating the four DNA binding sites. The predicted residues in the H/C link all appear in at least 1848 of the 2435 cases. We also note that the second binding site (position 15) is Serine in 1740 cases, but all the binding sites are clearly variable.

Clustering of genes. Figure 3 illustrates the tree for genes on the p arm of chromosome 19. The number after the human gene name locates the start of the gene in megabases. It is visually obvious that the tree structure reflects the geographic structure of genes on chromosome 19. For example, if we sever one arc of the tree then we separate the 23 genes that reside at 2.79-12.40 megabases from the 18 genes at 20.07-24.06 megabases. The probability we could get this result by cutting one of 40 arcs in the tree is at most $40/C_{41,23} = 1.98\times10^{-10}$, where $C_{41,23}$ is the number of ways of choosing 23 objects from a set of 41. There are 14 pairs of genes that are adjacent on the tree, i.e., both are connected to the same interior node. 11 of these 14 genes are adjacent on the chromosome suggesting tandem duplication events. If we keep the tree fixed and randomly reshuffle the labels then the probability we would see this pattern is at most

$$C_{14,11}\cdot(2/40)\cdot(2/38)\cdots(2/20) = 5.43\times10^{-11}.$$

Figure 4 shows zinc finger genes on the q arm of chromosome 19 that reside in the clusters at 49 and 58 megabases, which were earlier identified by Dehal et al. (2001). The ten zinc finger genes at 49.14-49.36 megabases are adjacent on the chromosome and

can be separated from the rest of the tree by cutting one arc, an event of probability at most $43/C_{44,10} = 1.73 \times 10^{-8}$. Tang, Waterman, and Yooseph (2002) studied the pattern of duplication in this cluster of human genes using specialized phylogenetic methods. Shannon et al. (2003) investigated this group of genes and also those that appear in the corresponding part of mouse chromosome 7, Zfp genes 61, 93, 108, 109, 111, and 235.

Figure 5 in Shannon et al. (2003) indicates the relationship between the last five Zfp genes and the trio Zfp61, ZNF226 and ZNF234 by representing fingers as boxes with various shading. That picture and the reasons for considering fingers to be similar become clearer if we list the α-helix sequence for each finger, the seven amino acid sequence containing the four binding sites as shown in Tables 2 and 3. A square bracket indicates a finger that has lost one of its critically important C, H, F or L residues, and a number indicates that insertions or deletions have changed the length from 28. As also indicated in Figure 5 of Shannon et al. (2003), Table 2 reveals that the fingers in columns 5-9 and 18-19 of Zfp61, ZNF226 and ZNF234 are closely related, while the fingers in columns 10-17 seem to have been added in the lineage leading to ZNF 226 and 234. To have genes with comparable fingers we choose ZNF 230, 222, 223, 221, 155, 224, and 225 to be cluster I.

Table 3 lays out the α-helix sequences for six of the genes considered in the left half of Figure 5 of Shannon et al. (2003), and two rat genes that Locus Link once reported as being orthologs of Zfp93 and Zfp108, but which have recently been removed as being "pseudogenes" (NCBI Help Desk email correspondence). Many of the relationships depicted in Table 2 of Shannon et al. (2003) are visible in ours. However, it is not clear why they concluded that the fingers in columns 17-19 of Zfp111 are

duplicates of those in columns 13-15, and are in turn homologous to columns 11-12 of ZNF235 and Zfp235, 93, and 108. To have similar finger structures we choose ZNF235, Zfp235, Zfp93, Zfp108, RNO308423, and RNO308422 to be cluster II.

We examined α-helix sequences for all of our zinc finger genes to identify other groups. Here and in what follows the numbers in parentheses indicate the start of the gene in megabases. As shown in Table 4, the α-helix sequences of ZNF440(11.78) and ZNF439(11.83) show strong signs of tandem duplication, as do ZNF44(12.22), LOC147837(12.28), ZNF442(12.36), LOC90576(12.36) and ZNF443(12.40). From the five intervening genes we choose ZNF20(12.10) to complete cluster III. Notice that these genes appear together in the tree in Figure 3. Our fourth and final cluster IV, consists of ZNF90(20.07), LOC163233(20.51), ZNF85(20.89), ZNF430(20.99), LOC148206(21.04), ZNF431(21.11), and LOC163227(21.69). These genes appear in two groups in the tree (Figure 3) but their α-helix sequences given in Table 5 are very similar to the others in the group.

In contrast to the four clusters considered above, one that occurs at the telomere of chromosome 19, which we will call Cluster V, has been very stable. Table 6 lists the NCBI annotated genes in this region and their orthologs in mouse and rat as given in NCBI's Locus Link. Apart from the somewhat unexpected location of Zfp35 on mouse chromosome 18 and of the AIBG orthologs on mouse chromosome 15 and rat chromosome 7, there has been little rearrangement. If one inverts the order of the last eight genes on the rat chromosome, then the order and orientation of the genes agree with the exception of the two FLJ's on lines 6 and 7. Figure 5 illustrates the relationship between genes in Table 6 as inferred by ClustalW. In contrast to the other clusters

considered earlier there is no evidence of duplication since the divergence of humans from rodents.

Tests for positive selection. Using the codeml program in PAML, we first applied the LRT M7 vs. M8 to our four zinc finger clusters. As Table 7 shows, we reject the null hypothesis of no sites under positive selection in clusters I, III, and IV, with the Bayesian posterior pointing to several sites potentially under positive selection. In the case of cluster IV, the test statistic is $2\Delta l = 2(l_{M8} - l_{M7}) = 47.910$, which is compared to χ^2 with df = 2, so $P < 0.0001$. Parameter estimates in cluster IV suggest that 5% of sites are under positive selection with $\omega = 6.58$. There are seven sites for which their posterior probability of $\omega > 1$ is greater than 0.95. Four of these appear at the first binding site (finger position 13) and three at the third binding site (16). In each of clusters I and III, PAML identifies a number of sites with posterior probability > 0.5 of positive selection but there is only one site with a significant (> 0.95) posterior probability of positive selection. These appear at sequence positions 1 (in the H/C link) in cluster I and 182 (finger position 14 in the binding region) in cluster III. The fitted values of ω in clusters I, III, and IV are 2.42, 1.53, and 6.58 respectively. To test if these are significantly > 1, we perform the LRT M8 vs. M8A. Clusters I and IV yield significant results, but cluster III just misses the cutoff with $P = 0.07$.

In our second analysis of these models, we divide the sites into constrained, binding, and unconstrained sites as described above. Results of the fixed-sites models are given in Table 8. It should not be surprising that model B which allows the mutation rate to vary between classes and model D which allows κ (transition/transversion ratio) and ω

to vary among partitions, in all cases emerge as significant improvements ($P < 0.001$) in the comparisons A vs. B and B vs. D.

Models C and E allow the amino acid frequencies to vary between classes. This introduces a large number of additional parameters, but paradoxically, in most cases results in fits that have a much worse likelihood than their simpler counterparts B and D. For example in cluster I, model C is 45.9 units worse than B and E is 43.8 units worse than D. Our best guess for the cause of this phenomenon is that when the sites are divided into classes, the observed frequencies of amino acids at the constrained sites differ considerably from the overall usage of amino acids in the protein and this causes trouble for the mutation model in PAML.

Model F is a separate analysis of the three partitions, i.e., it runs model A for each partition separately. As expected the estimated ω ratios at the constrained sites are small in all four clusters 0.20, 0.02, 0.16, 0.48 and the unconstrained sites are larger 0.66, 0.23, 0.55, and 0.48. For the class of binding sites we get ω values larger than 1 in clusters I, III, and IV: 1.14, 2.22, and 2.10. However, in cluster II our ω estimate is 0.34. To test if the values observed at the binding sites are significantly different from 1, we recalculate the log likelihood values in model F by fixing ω_1 to be 1, and perform the LRT as described above. Cluster I is not significant but clusters III, IV, and II are significant with P values 0.05, 0.01, and 0.001 respectively.

In the last analysis of our four clusters, we applied the parsimony based program ADAPTSITE.p (Suzuki and Gojobori 1999) to look for selection at individual codon sites. No positively selected sites are identified in any cluster, but several nonbinding

sites turn out to be under negative selection at the 5% significance level in clusters I (15 sites), II (24 sites), III (17), and IV (5 sites).

Results of our analysis using ADAPTSITE.p with data pooled by finger position are given in Table 9. There are three binding sites with significant positive selection, finger position 13 in Cluster III ($P < 0.0004$), and positions 16 and 19 in Cluster IV ($P < 0.0046$ and $P < 0.0458$ respectively), but only the first two are smaller than the threshold of 0.0178 demanded by the Bonferroni correction for our 28 tests. Again, there are a large number of nonbinding sites that show negative selection at this level. In cluster II this occurs for 21 of the 24 nonbinding sites, with four of the P values smaller than 10^{-6}. Indeed two of the binding sites, positions 15 and 16, show negative selection with P values < 0.0013 and < 0.00008 respectively, consistent with previous PAML analysis.

DISCUSSION

Our study of four clusters of zinc finger genes on human chromosome 19 has shown significant evidence for positive selection in cluster IV in all three analyses. In cluster III, the P values are borderline in the first PAML analysis (site-specific models), but significant in the second (fixed-sites models), and there is strong support for binding site position 13 being under positive selection in the third (parsimony analysis). In the case of cluster I, the significant result from the first test is not supported by the second and third. Finally, for cluster II, the second and third analyses show significant evidence of negative selection at the binding sites.

The results for cluster II are consistent with those of Shannon et al. (2003), who examined d_N / d_S ratios at three of the binding sites (our finger positions 13, 16, and 19) and found no evidence of positive selection in cluster II genes but significant evidence of purifying selection in pairwise comparisons of ZNF235 with Zfp235, Zfp93, and Zfp109, see their Table 2. In ZNF genes near our cluster I they find significant evidence of positive selection in comparisons of 226 with 230, 223, 284, and 222; 234 with 221; and 284 with 230. In no case are both of their compared genes within our cluster I (which consists of 155, 221-225 and 230). Some of the comparisons that Shannon et al. (2003) find significant are quite curious in view of the data presented in Table 2. ZNF223 has 9 zinc fingers versus 17 in ZNF226 and the overlapping fingers do not align well. ZNF284 and ZNF230 are more similar in length (11 versus 9 fingers) but comparison of the α-helix sequences reveals very little overall similarity.

Tandemly duplicated genes are subject to gene conversion events. Given the ability of gene conversion to homogenize gene families (see e.g., Chapter 11 of Li), it is natural to ask if concerted evolution can introduce correlated changes in different lineages and hence invalidates the use of Yang's and Suzuki and Gojobori's methods which assume independent substitutions. We cannot rule out the possibility that gene conversion acted soon after duplication to protect the duplicated copies from becoming pseudogenes (see Walsh 1987), an effect that can cause the underestimation of divergence times (see Teshima and Innan 2004). However, there are two reasons to doubt that this force has acted in the recent past.

First we observe that gene conversion acts to homogenize genes that perform the same function. Yet, Shannon et al.'s (2003) study of cluster I show that these genes have

different tissue specific expression patterns. The second obvious point is that if gene conversion is still acting, it is not doing a very good job. At a gross level, the numbers of zinc fingers of the genes in cluster I are 9, 9, 9, 15, 11, 19, and 17 respectively (the first three appear to be recent duplicates). Within clusters there is considerable divergence between sequences. For example in cluster IV, 23 synonymous and 36 nonsynonymous differences separate the 840 nucleotides in the most closely related pair (ZNF431 and LOC148206), and there are more than 100 differences between a typical pair of genes.

Several studies have presented evidence of gene conversion by examining patterns in the differences between genes and pointing out regions of unusually high similarity. See Figure 5 in Sharon et al. (1999), Figure 6 in Lazarro and Clark (2001), and Figure 6 in Bettencourt and Feder (2001). To look for similar signals in our data, we conducted an analysis (Figure 6) in which we calculated the number of nucleotide differences in a 168 nucleotide window (the length of two fingers) between adjacent genes in each cluster, advancing the window by 7 nucleotides until the end of the sequence is reached. Successive differences in each cluster are indicated by hollow squares, diamonds, and triangles, followed by filled versions of the symbols, and an X for the 7^{th} comparison. We find a lot of variability in divergence, but with the exception of one gene pair at the end of cluster III, no other regions dip below 5 nucleotide differences and most are above 10, which represents 6% divergence in the window. Assuming a mutation rate of 2×10^{-8} per nucleotide per generation, this suggests that gene conversion has not acted on these clusters in the last 3 million generations.

One of the disappointing aspects of our research is that although there are other groups of zinc finger genes on human chromosome 19 showing visible signs of a close

relationship, we have found only two new clusters of genes where positive selection can be demonstrated. There is a large group of genes near the centromere on the p-arm of chromosome 19 with no orthologs in rodents, but the reasons for the explosive growth of this gene family remain a mystery.

LITERATURE CITED

Bellefroid, E. J., D. A. Poncelet, P. J. Lecocq, O. Relevant, and J. M. Martial. 1991. The evolutionarily conserved Krüppel-associated box domain defines a subfamily of eukaryotic multifingered proteins. Proc. Natl. Acad. Sci. **88**:3608-3612.

Bellefroid, E. J., J. C. Marine, A. G. Matera, C. Bourginion, T. Desai, K. C. Healy, P. Bray-Ward, J. A. Martial, J. N. Ihle, and D. C. Ward. 1995. Emergence of the ZNF91 Krüppel-associated box-containing zinc finger gene family in the last common ancestor of the Anthropedia. Proc. Natl. Acad. Sci. **92**:10757-10761.

Benos, P. V., A. S. Lapedes, and G. D. Stormo. 2002. Probabilistic code for DNA recognition by proteins of the EGR family. J. Mol. Biol. **323**:701-727.

Bettencourt, B. R., and M. E. Feder. 2001. *Hsp70* duplication in the *Drosophila melanogaster* species group: How and when did two become five? Mol. Biol. Evol. **18**:1272-1282.

Choo, Y., and A. Klug. 1997. Physical basis of a protein-DNA recognition code. Curr. Opinion. Struct. Biol.**7**:117-125.

Dehal, P., P. Predki, A. S. Olsen et al. (21 co-authors). 2001. Human chromosome 19 and related regions in mouse: Conservative and lineage specific evolution. Science **293**:104-111.

Gell, D., M. Crossley, and J. Mackay. 2003. Zinc-finger genes. Pages 823-828 in Volume **5** of the *Nature Encyclopedia of the Human Genome.* MacMillan Publishers.

Innan, H. 2003. The coalescent and infinite-site model of a small multigene family. Genetics **163**:803-810.

Lander, E. S., L. M. Linton, B. Birren et al. (256 co-authors). 2001. Initial sequencing and analysis of the human genome. Nature **409**:860-921.

Lazzaro, B. P., and A. G. Clark. 2001. Evidence for recurrent paralogous gene conversion and exceptional allelic divergence in the *Attacin* genes of *Drosophila melanogaster*. Genetics **159**:659-671.

Li, W. H. 1997. Molecular Evolution. Sinauer, Sunderland, MA.

Looman, C. 2003. *The ABC of KRAB Zinc Finger Proteins.* Comprehensive Summaries of Uppsala Dissertations, **864**. Acta Universitatis Upsalenis.

Looman, C., M. Åbrink, C. Mark, and L. Hellman. 2002. KRAB zinc finger proteins: An analysis of molecular mechanisms governing their increase in complexity during evolution. Mol. Biol. Evol. **19**:2118-2130.

Margolin, J. F., J. R. Friedman, W. K. Meyer, H. Vissing, H. J. Thiesen, and F. J. Rauscher, III. 1994. Krüppel-associated boxes are potent transcriptional repressor domains. Proc. Nat. Acad. Sci. **91**:4509-4513.

Miller J., A. McLachan, and A. Klug. 1985. Repetitive zinc-binding domains in the protein transcription factor IIA from Xenopus oocytes. EMBO J. **4**:1609-1614.

Nielsen R., and Z. Yang. 1998. Likelihood models for detecting positively selected amino acid sites and applications to the HIV-1 envelope gene. Genetics **148**:929-936.

Schuh, R., W. Aichler, U. Gaul et al. 1986. A conserved family of nuclear proteins containing structural elements of Krüppel, a Drosophila segmentation gene. Cell **47**:1025-1032.

Shannon, M., A. T. Hamilton, L. Gordon, E. Branscomb, and L. Stubbs. 2003. Differential expansion of zinc-finger transcription factor loci in homologous human and mouse gene clusters. Genome Research **13**:1097-1110.

Sharon, D., G. Glusman, Y. Pilpel, M. Khen, F. Gruetzner, T. Haaf, and D. Lancet. 1999. Primate evolution of an olfactory receptor cluster: Diversification by gene conversion and recent emergence of pseudogenes. Genomics **61**:24-36.

Swanson, W. J., R. Nielsen, and Q. Yang, 2003. Pervasive adaptive evolution in mammalian fertilization proteins. Mol. Biol. Evol. **20**:18-20.

Tang, M., M. Waterman, and S. Yooseph. 2002. Zinc finger clusters and tandem gene duplication. J. Comp. Biol. **9**:429-446.

Teshima, K. M., and H. Innan. 2004. The effect of gene conversion on the divergence between duplicated genes. Genetics **166**:1553-1560.

Thompson, J. D., D. G. Higgins, and T. J. Gibson. 1994 CLUSTAL W: improving the sensitivity of progressive multiple sequence alignment through sequence weighting, position specific gap penalties and weight matrix choice. Nucleic Acids Research **22**:4673-4680.

Venter, J. C., M. D. Adams, E. W. Myers et al. (274 co-authors). 2001. The sequence of the human genome. Science **291**:1304-1351.

Walsh, J. B. 1987. Sequence-dependent gene conversion: Can duplicated genes diverge fast enough to escape conversion? Genetics **117**:543-557.

Wolfe, S. A., L. Nekludova, and C. O. Pabo. 1999. DNA recognition by Cys2His2 zinc finger proteins. Annu. Rev. Biophys. Biomol. Struct. **3**:183-212.

Wong, W. S. W., Yang, Z., Goldman, N., and Nielsen, R. 2004. Accuracy and power of statistical methods for detecting adaptive evolution in protein coding sequences and for identifying positively selected sites. (to appear)

Yang, Z. 1997. PAML: a program package for phylogenetic analysis by maximum likelihood. CABIOS **13**:555-556. http://abacus.gene.ucl.ac.uk./software/paml.html.

Yang, Z., R. Nielsen, N. Goldman, and A. M. K. Pedersen. 2000. Codon-substitution models for heterogeneous selection pressure at amino acid sites. Genetics **155**:431-449.

Yang, Z., and W. J. Swanson. 2002. Codon-substitution models to detect adaptive evolution that account for heterogeneous selective pressures among site classes. Mol. Biol. Evol. **19**:49-57.

	25	26	27	28	1	2	3	4	5	6	7	8	9	10
	T	G	E	K	P	Y/F		C			C			
A	86	64	33		24		71		39	40		18		**1237**
L	13		15		86	12			16	34				38
I	47	11	12				64		33	57				12
V	20	26	48				117		26	189				171
P	15		12		**2054**		14		60					10
F					15	**324**								49
W														
M	26						22		19					
G	15	**2012**	43	31	10		37		87			**2106**		**244**
S	257	22	12		99		17		259	14		33		**331**
T	**1848**	13	11	23	30		60		76	42				**169**
Y						**1933**				13				
C					14	37		**2435**			**2435**			35
N	25			39			35		359	12			18	10
Q		20	45	26	13		96		73	272		21	43	
D		22	77				43		157	144		93		20
E	11	86	**1959**				656		546	**1419**		44	31	24
K	19	27	128	**1953**			1060		591	128		24	**2195**	
R	19	98	17	316	40		102		51	17		48	111	65
H	14				22	93	18		30	39				

	11	12	13	14	15	16	17	18	19	20	21	22	23	24
	F		*		*	*	L/F		*	H				H
A		56	12	92	140	140		162	147			54	23	
L		36	80	84	32	52	**2212**	132	96		108	28	75	
I		162	19	35	14	65		345	196		21	214	**1185**	
V		39	74	39	11	47		135	212		46	80	460	
P		17		144	32	12								
F	**2435**	22	41	104	38	22	**223**	35					20	
W			162								30			
M		26	30	14				32	33		63	35	38	
G		97	28	122	69	75			48		18	38	10	
S		791	165	799	**1740**	441		152	103		11	49	90	
T		261	39	44	127	256		616	252		24	50	458	
Y		21	181	53	53	158		16	37		14			
C		56	142	36	21	56			29		20		10	
N		318	62	174	24	326		127	81			20	31	
Q		12	639	35	29	140		255	327		998	26		
D		11	47	22	10	81		17	38				10	
E			43	10	16	24		24	134		247			
K		124	65	287	22	68		84	285		506	301		
R		333	381	253	29	81		203	366		224	**1514**	13	
H		53	225	82	17	385		84	39	**2435**	80			**2435**

Table 1. Amino acid counts for the 2435 fingers in the 222 genes in our data set. For clarity numbers smaller than 10 are omitted.

	1	2	3	4	5	6	7
ZNF284			qnsqlqt	rrsgmyv	hnsqlre	srsnlnr	qrsalns
ZNF230		yisalri	qssclqt	crailqv	hdlklqk	lrsslnr	dsldlhk
ZNF222		yisalhi	qssrlqt	crsalkv	hnfqlqk	lrsslnr	[drldlhk]
ZNF223		yisalhi	qslhlqt	crsaltv	hdfqlqk	lrsslnr	[drldlhk]
ZNF221	dvsvfdl	yspalhi	qsshlqt	[srsalnv]	hdsqlqe	vrsrlnr	qrsalns
ZNF155		yisalhv	qsshlqt	rrsalnv	hdsqlke	frsrlks	qrsalnr
ZNF224		yisalri	qsshlqt	rrsalnv	hdsqlqe	grsrlnr	qrsalns
ZNF225		yssalri	qsshqqi	rrsglyv	hdsqlqe	sranlnr	lksalns
ZNF234		yisalhi	qsshlqt	rrstltv	hashlqe	rrsalnn	cssnlri
ZNF226			qgahlqt	rrsalnv	qashlqd	rnshlqs	cssnlyi
Zfp61				vdqhlms	qashlqd	rsshlrs	cssnlyi

	8	9	10	11	12	13	14
ZNF284	crqdlck	wssclsr	[mnsqghs]	skfnldl	wasgilr	ensklrf	
ZNF230	wssylli	sksglnl	rassiln				
ZNF222	wssyllv	sksgldf	hassiln				
ZNF223	wssyllv	sksgldl	qassiln				
ZNF221	crrdfck	wsscln	tnsrrss	rrldlef	wascllk	qstqlhs	skfnldm
ZNF155	grldfyk	wsscln	tnsqlss	tkfnldl	rassiln		
ZNF224	crrdlyt	wascllk	tnsqcys	rrldldf	rapcllk	qnshlhs	skfnldm
ZNF225	yrqdlyk	wasglsr	tnsqrys	rrldldf	wascln	qnsqlyt	qnsqlys
ZNF234	qpsqfqa	ysssfqa	mkihyqv	qssylki	qssrlqi	rradlki	qashllt
ZNF226	rpsslqa	lssnlqa	rnshyqv	qssylqi	qssrlqi	rradlki	qasnlla
Zfp61	rpsslqa	lnsnlqv					

	15	16	17	18	19	20
ZNF221	wascllk					
ZNF224	[wascllk]	qnsqlhs	wsstrlt	[qnsfskv]	rrlnldm	qasslrl
ZNF225	skfnldm	rassiln	ensqlhs	wasthlt		
ZNF234	rsahlqa	wslnldm	qasslql	rssqlqy	wrsnlvs	
ZNF226	rsahlqa	wslnldm	qasslql	rssqlqs	wrsnltv	
Zfp61				rssqlqs	wrsnlii	

Table 2. Alpha helix sequences for the cluster of human zinc finger genes at 49 megabases on chromosome 19, including cluster I. Here and in the next three tables, brackets indicate fingers that have lost one of the critical C, H, F or L residues, and numbers indicate fingers with length different from 28 amino acids.

	1	2	3	4	5	6
Zfp109	qssalqt	qwsvlha	fssnlhi	26	sasnvkv	rsfhlht
ZNF235	qssnlqt	qsshlya	rstdlni	qrshlqa		cssnlht
Zfp235	qssnlqt	qsshlya	rstdlni	qrshlqa		cssnlht
Zfp93	qssalqt		rssdlni	qwahlqa		cssnlht
RNO308423	hsstlqt		rssdlni	qwahlqa		cssnlht
Zfp108	hsstlqt		rssdlni	kwdhlqi		[cswnlht]
RNO308422	qssalqt		rnsdlni	kwdhlqi		cswnlht
Zfp111	qssalqt		[rssdlni]	qcsllqa	cisnfhi	27
RNO292703	qssalqt		[rssglsi]	rwshlqa	cisnlht	lnfnlhi

	7	8	9	10	11	12
Zfp109	qrsslqv	sassfqg	rssylqi		qrahlqv	qrsglss
ZNF235	lsfnlhs	sassfqs	qssyfqa	wslnlhn	qasnlqa	qashlqa
Zfp235	lsfnlhs	sassfqs	qssyfqa	wslnlhn	qasnlqa	qashlqa
Zfp93	lsgnldi	sassfqs	rsshfld	wslslhs	hasslqa	ktsnlqa
RNO308423	lsgnldi	sassfrg	rsshfld	wslslhs	hasslqa	kasnlqa
Zfp108	lsfnlhs	sassfqr	qssnfqa	26	hasslqa	qasilqd
RNO308422	lsfnlhs	sassfqr	qssnfqa	26	hawslqv	qasilqd
Zfp111		sassfqr	rtsylqt		qlshlqa	cssnlht
RNO292703	lsfnlhs	sassfqr	[rdsnlqt]	csmdlni	ylshlqa	yssnlht

	13	14	15	16
Zfp109	qpslfer	qrshlvk		
ZNF235	qrsnlqv	wsaglsa	qashfht	qrshliy
Zfp235	qrsnlqv	wsaglta	qashfht	qrshlvy
Zfp93	qksslqv	wsvglss	qasyfhm	
RNO308423	qrsslqv	wsaglta	qasyfht	qashfht
Zfp108	qrsglqv	wnsglss	qashfht	
RNO308422	qrsglqv			
Zfp111	[lvsglqa]	qawnlha	qrsglqi	lnsglia
RNO292703	[lasslqa]	qawnlqa	qrsslqi	lnsglta

	17	18	19	20
Zfp111	lasslrt	qvshlqs	qksglqv	wssglsa
RNO292703	lasslrt	qvshlqs	qksglqv	wssglsa

Table 3. Alpha helix sequences for mouse and rat genes that are related to ZNF235, including cluster II.

	1	2	3	4	5	6
ZNF440	shssvrr	clrlyli	ysathri	[sprsyrr]	cpryvri	sltsfqt
ZNF439	yhssiqr	clslyli	ysathri	sprschr	cpryvrr	sltsfqt
ZNF20	flnlcli	rsttlpv	fpseirr	sfssiqy	cgshlqk	ctsdlqr
ZNF44	wpsllrm	vyssylr		dyssylr	vsgslrv	hlgsfqr
LOC147837	wpsllrm	fyssyrr		dsssyir	vssslrr	hlgsfqi
ZNF442	wpslfrm	iyssylr		dyssyvr	vssslri	hlgsfqr
LOC90576	wpsllhm	fyssylr		dyssclr	astslrr	hlgsfqr
ZNF443	wpsllhm	fyssylr	fyssylr	dsssCli	vsgslqr	hlgsfqr

	7	8	9	10	11	12
ZNF440	svnsfqr	hssslry	sashlrv	34	cpksfqr	
ZNF439	saksfqr	rsgsfry	sapnlql	sasqlri		
ZNF20	casqlqi	yfsslri	yfsslhi	csssiry		
ZNF44	fpgsari	hrssfrr	spsvfqr	tssslrk	27	sfkyfcr
LOC147837	rpslvry	hsssfrr	ypsvcqr	hsssfrr	ypsvcqr	
ZNF442	cpsslqs	hhssfrs	ypsvfqg	issslrr	27	cftylsq
LOC90576	cpsslks	hsssfrr	ypsvfqr	issslrr	27	cfqylsq
ZNF443	cpsslqs	hrssfrs	ypsvfqr	issslrr	27	rfrylsr

	13	14	15	16		17
ZNF44	rfsylkt	wpsfllr	rssfcre			
ZNF442	hfgnlkv	wltcllr	rsrflrg			
LOC90576	hfgnlkv	wltcflr	hsrflqg	slsslhr		slsslhr
ZNF443	hydnlkv	wltcflr	hsrflqg	slsslhr	5	slsslhr

Table 4. Alpha helix sequences of Cluster III.

	1	2	3	4	5	6
ZNF90	qsstlat	rsshlts	ysstlta	ysstlta	sssilyv	lssilst
LOC163233	qsstltt	wsshltt	rfsylta	rssnltt	rssilta	hpsvltt
ZNF85	misclte	wsstltk	qssnlik	rfstltt	rsstltt	qssnltt
ZNF430	mllhltq	wfstltr	qsstltt	rsshltt	rsshltt	qsstltt
LOC148206	mllhlhq	rfstltr	hsstltt	hsshltt	hpsaltt	rfsyltk
ZNF431	mllhlsq	wfstltr	qsstltt	rsshltt	qsstlst	rfsyltk
LOC163227	mllhltq	wfstltt	rsshltt	rsshltt	rsshltt	qsstltt

	7	8	9	10	11	12
ZNF90	rslvlrt	sssllyk	rsstlti	rssalst	rssnltt	yssalst
LOC163233	yfssltt	wsshltt	ysssltt	cfsiltt	ssshlta	rsfiltr
ZNF85	qsahltt	hfshltt	hsstltk	[qssklte]	qssnltr	wpstlti
ZNF430	rfsyltk	wsstltk	essnlta	rspklta	qfsnltk	
LOC148206	wsstltk	vsshltt	hssklti	qssnltk	rssnltt	rssnltk
ZNF431	wsstltk	essnltt	rspqlta	qssiltt	rssnltk	qsstltk
LOC163227	rfsylik	wssaltk	essnltt	rssqlta	rsstltk	

	13	14	15
ZNF90	rssvlsk	rssqlts	lssdlnt
LOC163233	cpstltt		
ZNF85	qsskltk	qssnltk	wssvltk

Table 5. Alpha helix sequences of Cluster IV.

	Human gene	Mouse gene		Rat gene	
63.161 -	MGC41906	2900092C05Rik	7-9.674 –		
63.180 -	FLJ14260	2410024M24Rik	7-9.768 -	LOC292610	1-72.660 +
63.215 -	LOC376552				
63.237 +	FLJ33779				
63.270 +	ZNF135	Zfp35	18-24.530		
63.287 -	FLJ12895	LOC232875	7-10.095 -	LOC292615	1-73.191 -
63.329 -	FLJ12586	2810439M05Rik	7-10.386 +	LOC308361	1-72.777 -
63.382 +	ZNF274	Zfp110	7-10.336 +	LOC308362	1-72.813 +
63.419 +	LOC125910				
63.432 +	AF20591				
63.482 +	ZNF8	Zfp128	7-10.118 +	LOC308363	1-72.866 +
63.530 +	HKR2	D530006B18Rik	7-10.135 +	LOC308364	1-72.890 +
63.548 -	A1BG	LOC223599	15-62.029	A1bg	7-97.803
63.559 -	LOC162968				
63.570 -	LOC116412				
63.590 +	RPS5	Rps5	7-10.159 +	Rps5	1-72.906 +
63.602 -	FLJ39005				
63.611 +	LOC201514				
63.636 -	ZNF132	Zfp132	cyto only		
63.670 +	ZF5128	D430030K24Rik	7-10.218 +	LOC365192	1-73.032 -
63.679 +	FLJ20626	A630035I11Rik	7-10.230 +	LOC308365	1-73.022 -
63.701 -	SLC27A5	Slc27a5	7-10.240 -	LOC79111	1-73.002 +
63.716 -	FLJ14486	LOC232879	7-10.258 -	LOC308366	1-72.990 +
63.747 +	TRIM28	Trim28	7-10.275 +	Trim28	1-72.970 -
63.754 -	BC-2	1500016L11Rik	7-10.283 -	LOC365191	1-72.968 +
63.758 -	UBE2M	Ubc-rs2	7-10.286 -	LOC361509	1-72.963 +
63.765 -	ZNF42	Zfp98	7-10.294 -	LOC361508	1-72.931 +

Table 6. Cluster V and orthologous genes in mouse and rat. Positions are indicated in megabases, with the first number in the mouse and rat columns specifying the chromosome and signs giving the orientation of the gene.

Model	**Cluster I**	**Cluster II**	**Cluster III**	**Cluster IV**
M7 (beta)	-3005.662	-2654.088	-3483.110	-3172.882
M8A	-3004.938	-2653.128	-3480.784	-3167.185
M8 (beta & ω)	-3002.171 $p_1 = 0.074$ $\omega = 2.419$	-2652.101 $p_1 = 0.004$ $\omega = 16.143$	-3479.158 $p_1 = 0.195$ $\omega = 1.526$	-3148.927 $p_1 = 0.052$ $\omega = 6.582$
M7 vs. M8	**$2\Delta l = 6.982$** ***P* < 0.05**	$2\Delta l = 3.974$ $P = 0.14$	**$2\Delta l = 7.904$** ***P* < 0.05**	**$2\Delta l = 47.910$** ***P* < 0.0001**
M8 vs. M8A	**$2\Delta l = 5.534$** ***P* < 0.05**	$2\Delta l = 2.054$ $P = 0.15$	$2\Delta l = 3.252$ $P = 0.07$	**$2\Delta l = 36.516$** ***P* < 0.0001**

Table 7. Log-likelihood values and fitted parameters for site-specific models. For each LRT, $2\Delta l$ is compared to χ^2 with df = 2. Boldface indicates significant results.

Model	**Cluster I**	**Cluster II**	**Cluster III**	**Cluster IV**
A (homogeneous)	-3046.741	-2681.407	-3555.517	-3233.715
B (different rs)	-3028.001	-2670.099	-3505.481	-3138.739
C (different rs & πs)	-3073.979	-2674.725	-3551.098	-3140.110
D (different rs, κ and ω)	-3011.958	-2634.975	-3473.532	-3110.030
E (different rs, κ and ω, & πs)	-3055.735	-2634.275	-3521.239	-3112.362
F (separate analysis)	-3040.904	-2608.443	-3497.644	-3092.701
	Binding sites: -495.440	Binding sites: -467.418	Binding sites: -614.180	Binding sites: -669.518
	Fixing ω=1: -495.535	Fixing ω=1: -475.595	Fixing ω=1: -616.614	Fixing ω=1: -702.968
	$2\Delta l = 0.190$ $P \sim 0.66$	**$2\Delta l = 16.354$** **$P < 0.001$**	**$2\Delta l = 4.868$** **$P < 0.05$**	**$2\Delta l = 6.900$** **$P < 0.01$**
ω_1 (binding sites)	1.14	0.34	2.215	2.10
ω_2 (constrained sites)	0.20	0.02	0.160	0.14
ω_3 (all else)	0.66	0.23	0.545	0.48

Table 8. Log-likelihood values for fixed-sites models and fitted values of $\omega = d_N / d_S$. Here the LRT focuses on the binding sites analyzed using model F where $2\Delta l$ is compared to χ^2 with df = 1. Again boldface indicates significant results.

		I	II	III	IV
4	C		0.000021	0.000025	
7	C		0.000004		
20	H	0.000017	0	0.000017	0.001372
24	H	0		0.000092	
11	F	0.000012	0.001372	0.000032	0
17	L		0		
25	T		0		
26	G		0.000007		
27	E	0.001895	0.000012		0.008111
28	K	0.000072	0.000001		
1	P		0.000001	0.000409	0.011906
2	Y		0.000162		
3			0.011503		
5		0.016277	0.009948	0.000001	
6		0.017349	0.00074	0.002185	
8			0.005389	0.003090	0.011941
9		0.001263	0		
10				0.015824	0.000075
12			0.001935		
14			0.004581		
18			0.000068		
21					0.001331
22			0.006919		
23			0.011867		
13	*	0.590508	0.840180	**0.000375**	0.665060
15	*	0.695631	0.999695	0.163579	0.983200
16	*	0.755179	0.999989	0.742808	**0.004593**
19	*	0.288510	0.956726	0.095662	**0.045765**

Table 9. One sided *P* values for negative selection at nonbinding sites and positive selection at binding sites. All *P* values are given for binding sites but in other cases only *P* values significant after Bonferroni correction are shown. Here 0 indicates a *P* value smaller than 10^{-6}. Boldface indicates significant results for positive selection.

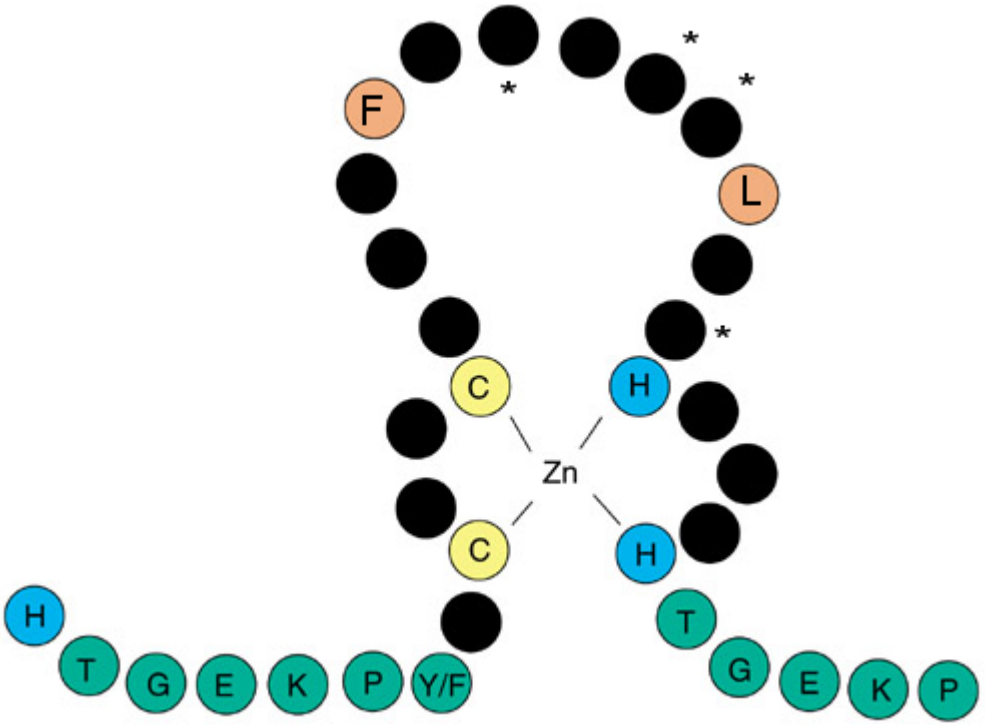

Figure 1. Structure of a zinc finger. Stars indicate sites involved in DNA binding.

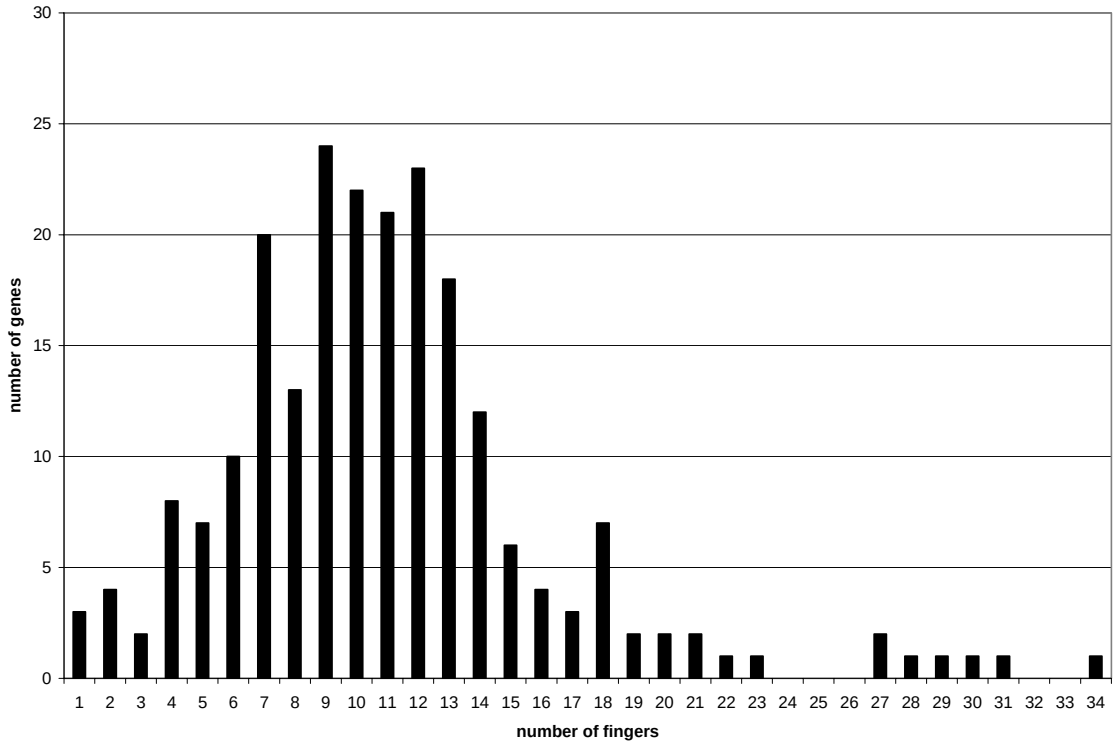

Figure 2. Histogram of the number of fingers in the 222 genes in our data set.

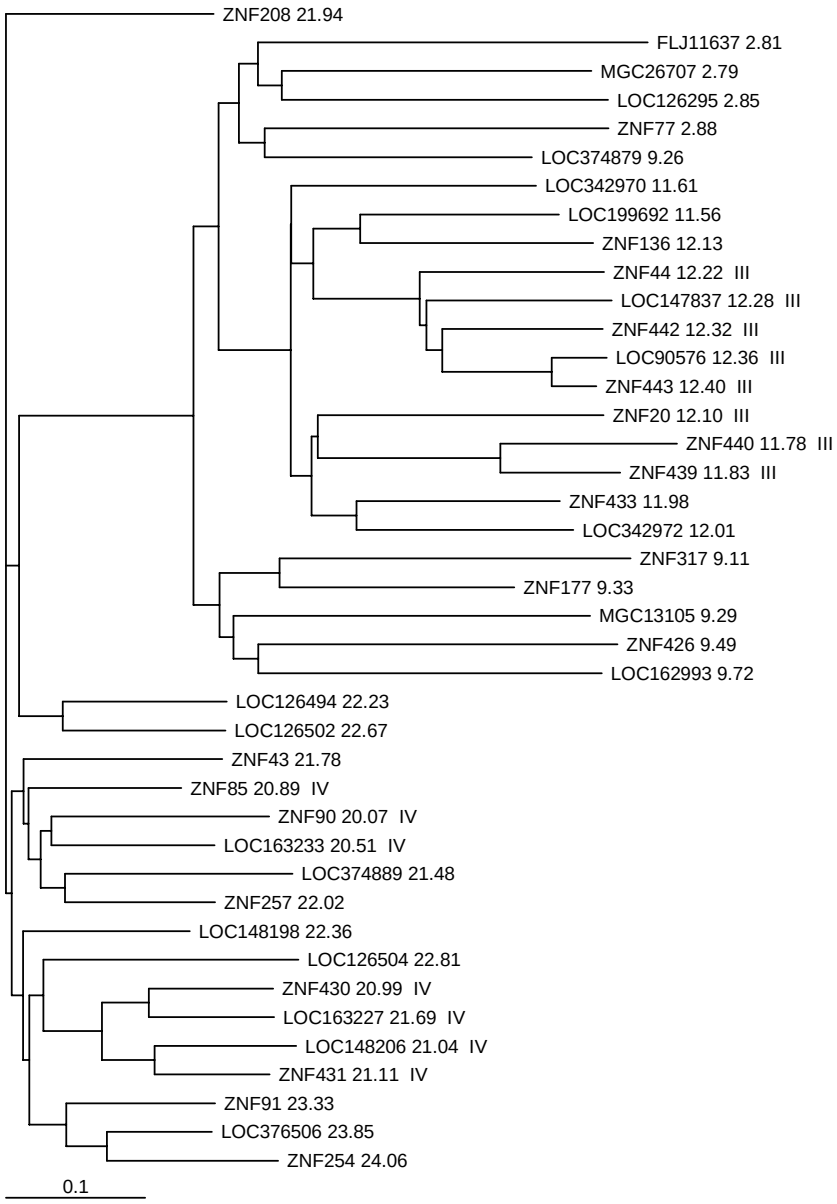

Figure 3. Tree for KRAB containing zinc finger genes on human chromosome 19p. Numbers give their chromosomal location in megabases. Clusters III and IV are indicated. Note the close relationship of genes at 20-24 megabases.

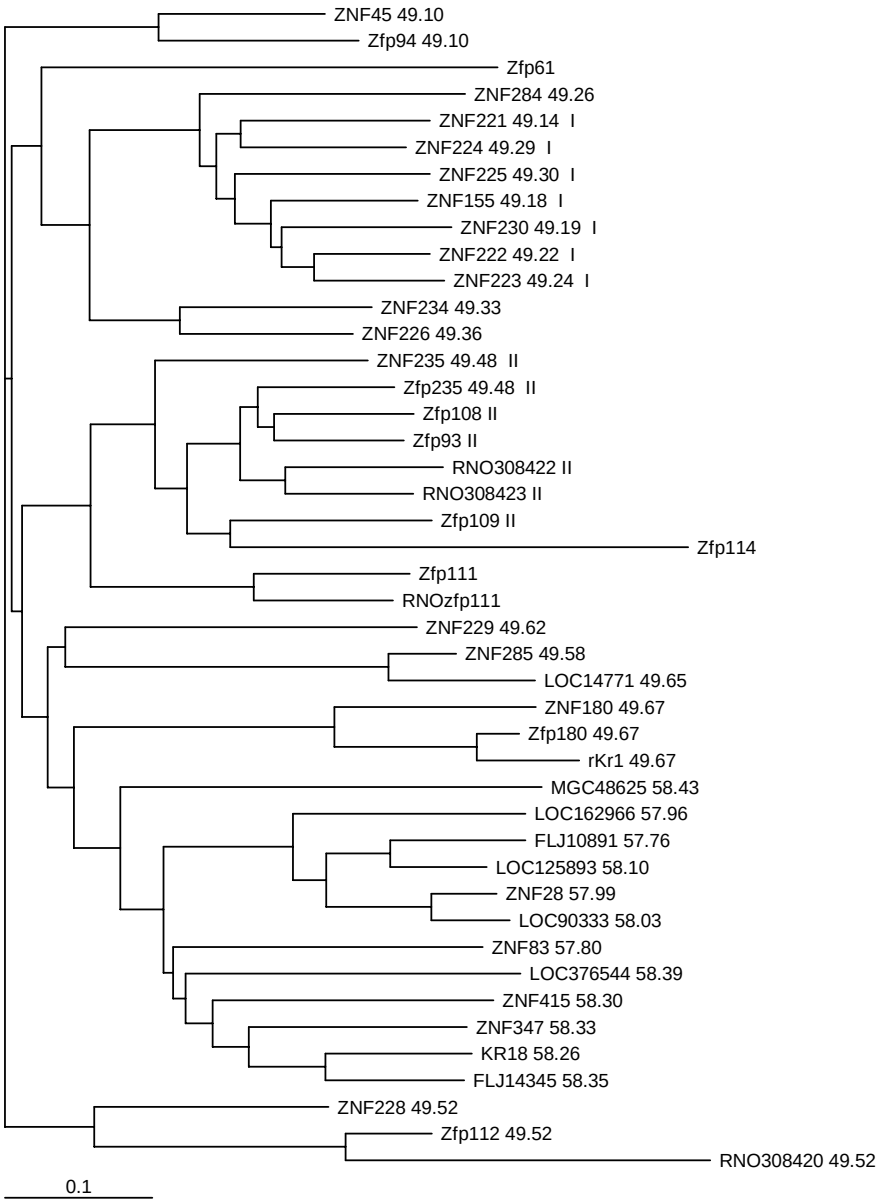

Figure 4. Tree for zinc finger genes in clusters at 49 and 58 megabases on human chromosome 19q along with related mouse and rat genes. Numbers give their chromosomal location in megabases of the gene or of its human ortholog. Clusters I and II are indicated.

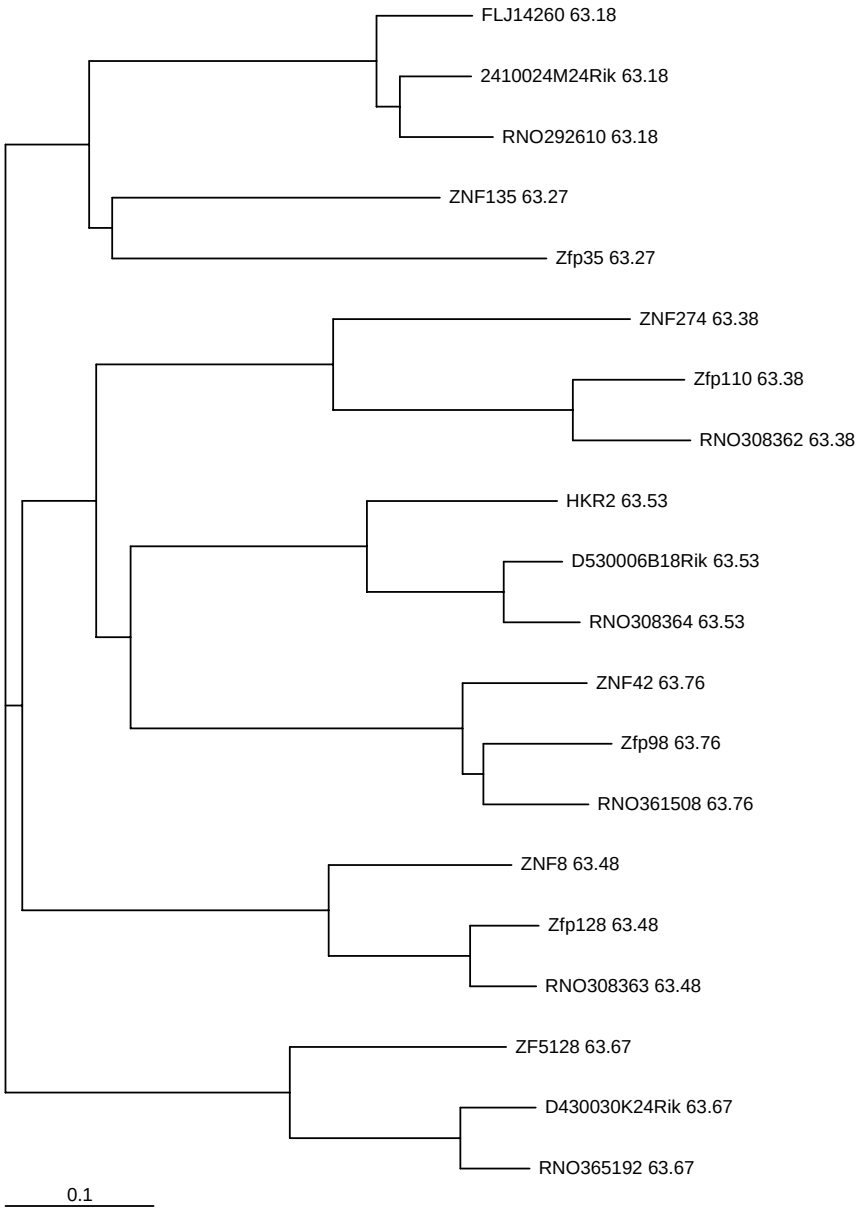

Figure 5. Genes near the telomere of human chromosome 19 that have orthologs in rat and mouse. Human genes are numbered by their chromosomal location in megabases, rat and mouse genes by the location of their human ortholog. The structure of the tree suggests that all of these genes were present in the common ancestor of humans and rodents.

Cluster I

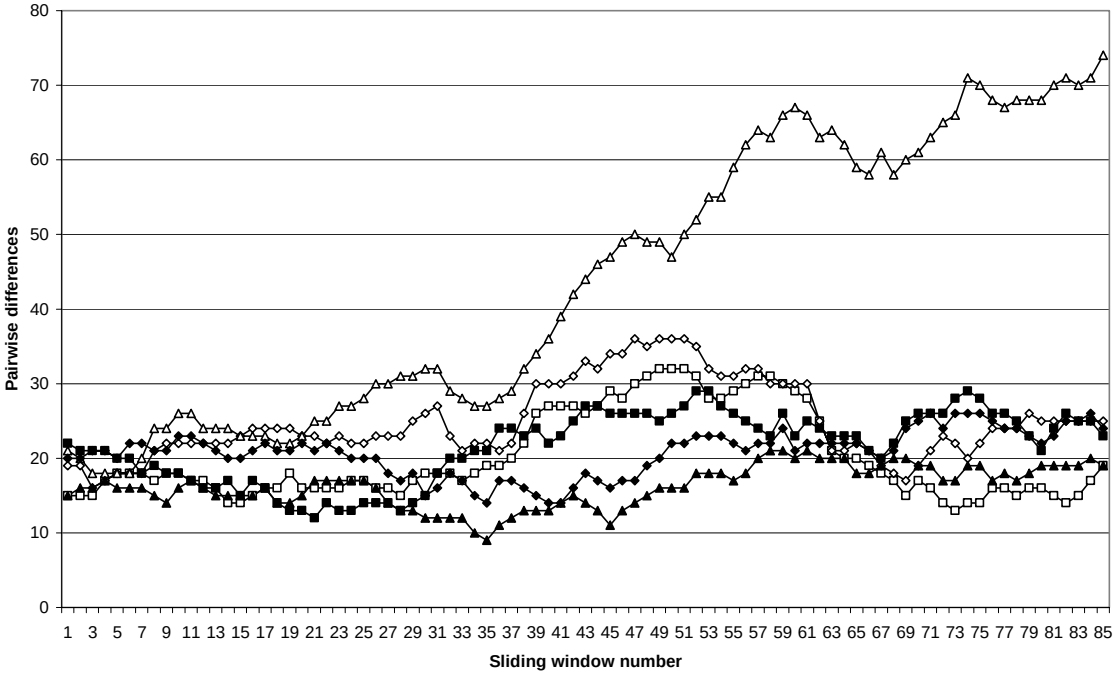

Cluster II

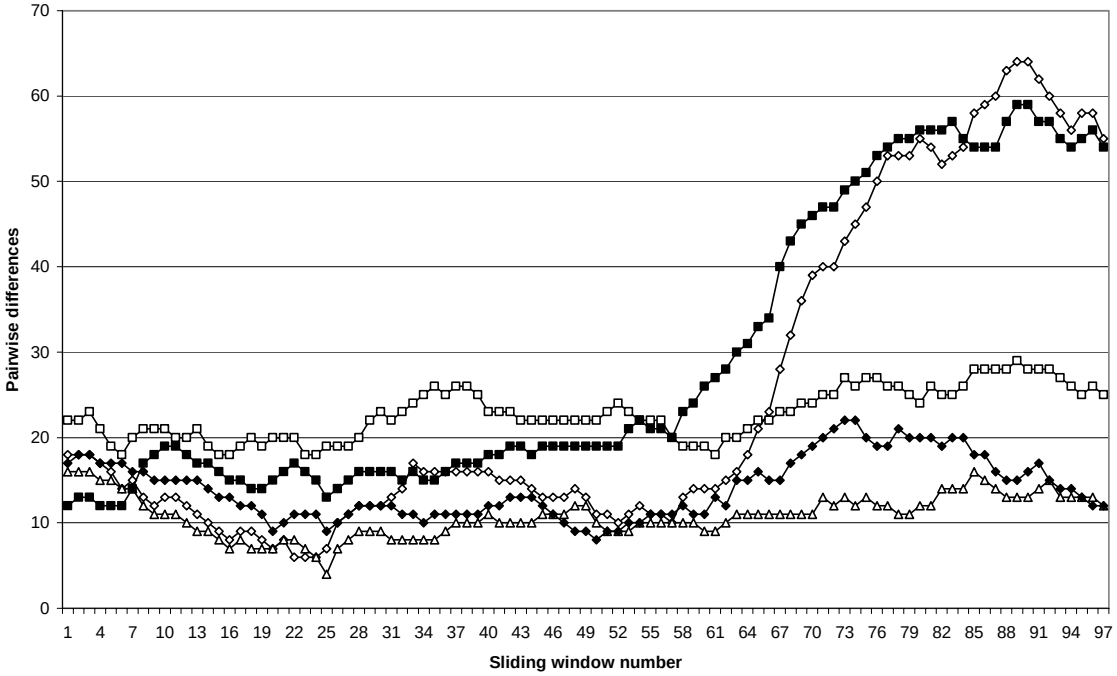

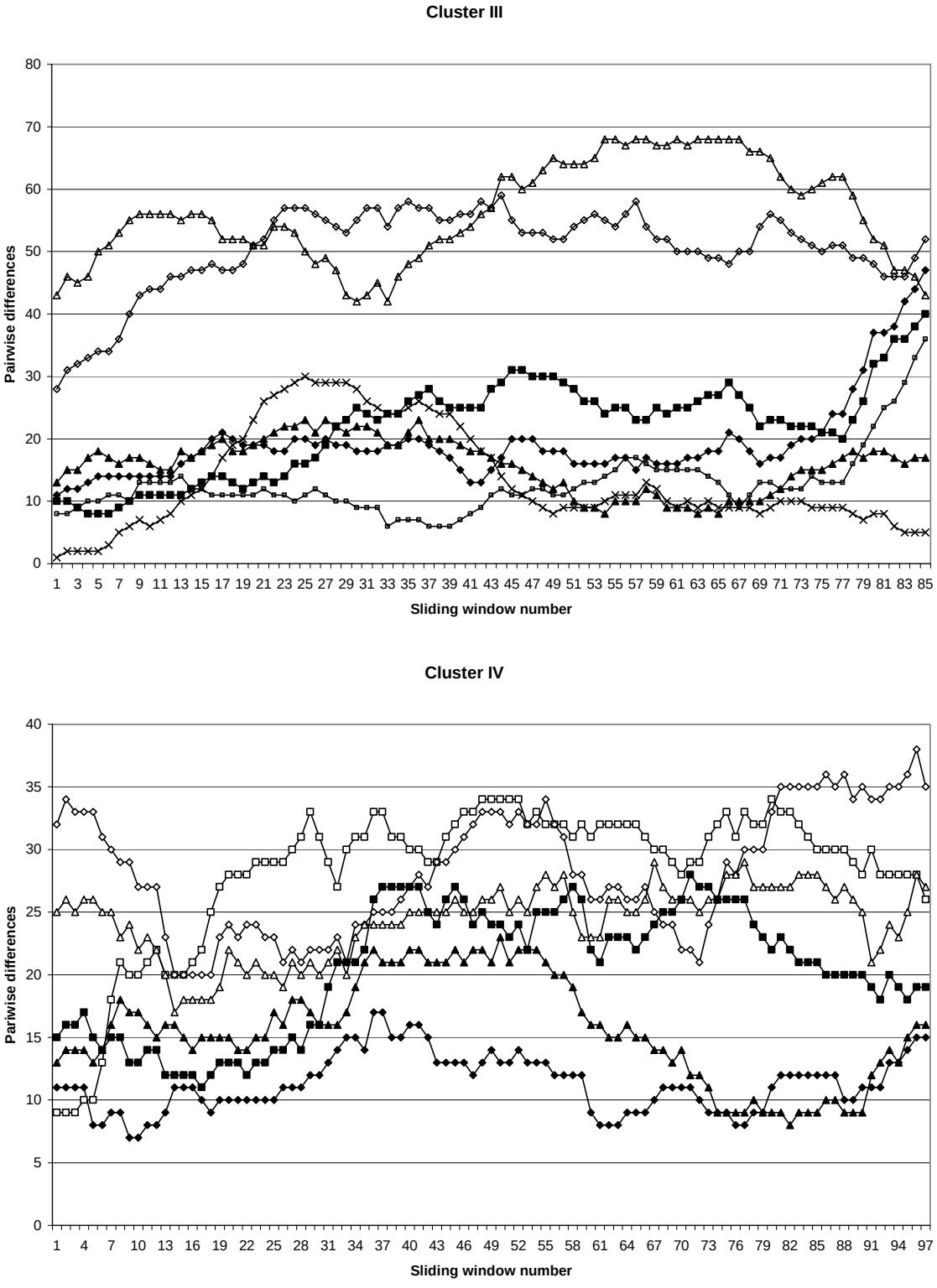

Figure 6. A sliding window analysis calculates the number of nucleotide differences between successive sequences in the cluster. We use a 168 nucleotide window (the length of two zinc fingers) that advances by 7 nucleotides in each step.